

QUALITATIVE BEHAVIORS AND CONTROL OF A NEW FOUR-DIMENSIONAL LORENZ SYSTEM

Fuchen Zhang^{1,†}, Song Chen¹, Xiusu Chen¹, Fei Xu² and Min Xiao³

Abstract. In this paper, a new nonlinear four-dimensional Lorenz system is proposed. Nonlinear dynamical properties of this system, including the stability of the fixed points, Lyapunov exponents, the bifurcation behaviors and sensitivity to initial conditions, are considered by using chaos theory and numerical simulations. It is very interesting that we find that this system exhibits chaos phenomena for a new set of parameters. The global exponential attractive set of this system has been obtained according to Lyapunov stability theory. Synchronization has been realized between two identical hyperchaotic systems via globally exponential approach and sliding mode control method by using the results of the global exponential attractive set, Vaidyanathan's theorem and Dini derivative. The novelty of the paper lies in that the global exponential attractive set of the system is obtained firstly, then the result of the global exponential attractive set is used to study chaos control and chaos synchronization. Furthermore, the precise mathematical expression of the controller is obtained according to the boundedness of this system. Finally, the synchronization process is simulated by MATLAB to illustrate the effectiveness of the theoretical analysis. The results of numerical simulations show that two control methods for chaos synchronization are effective.

Keywords: Lorenz system, stability theory, qualitative theory, global exponential synchronization, sliding mode control.

MSC(2010) 34D06, 34H10, 26A33, 39A13.

1. Introduction

Unpredictability is a phenomenon in nonlinear dynamics that discovered by Henri Poincaré [1] who is a famous scientist and mathematician in the world when he studied the three-body problem: earth, moon, and sun move under their mutual gravitational interactions. He found that a small change in the initial condition of this problem can cause a large error in the final phase that would become known as chaos. However, Poincaré's results did not attract much attention at the time. In 1975, Li and Yorke [2] coined the mathematical, physical concept of "chaos" which is known as "Li-Yorke chaos". In 1963, the meteorologist E.N. Lorenz [3] built nonlinear weather models to predict the weather forecast and he found that this nonlinear system could exhibit very complex behaviors and chaos due to the sensitive dependence upon the initial conditions which is known as the butterfly effect. The scientific gateway to chaos research was reopened.

[†]The corresponding author.

¹School of Mathematics and Statistics, Chongqing Key Laboratory of Statistical Intelligent Computing and Monitoring, Chongqing Technology and Business University, Chongqing 400067, China

²Department of Mathematics, Wilfrid Laurier University, Waterloo, Ontario N2L 3C5, Canada

³College of Automation & College of Artificial Intelligence, Nanjing University of Posts and Telecommunications, Nanjing 210023, China

Email: zhangfuchen1983@163.com(F. Zhang), fxi.feixu@gmail.com(F. Xu), candymanxm2003@aliyun.com (M. Xiao)

Since then, chaos phenomena arising from nonlinear systems have attracted much attention from many scientists. To discover new chaotic systems for exploring the mechanism of chaos is an important research direction of chaos research. In 1976, the Rossler system was discovered [4]. In 1986, the Chua circuit system was found by Leon O. Chua in a physical experiment [5, 6]. In 1996, the Swedish physicist Stenflo [7] established a four-dimensional Lorenz system to describe the dynamics of acoustic-gravity waves, namely, the Lorenz-Stenflo system. In 1999, Chen and Ueta found a new chaotic system, namely, the Chen system [8]. In 2002, Lu and Chen found a novel chaotic system which connected the Lorenz system and the Chen system [9]. In 2002, Lu et al. introduced the unified chaotic system [10]. Since then, many chaotic systems have been discovered and studied [11-22]. Chaos phenomena have been found and studied in encrypted communication, biology, engineering technology, neural network, fluid mechanics and other fields by many researchers [11-23].

The technique for controlling chaos is predictive control and synchronization control. The phenomenon that the dynamical behaviors of two chaotic systems become consistent is known as chaos synchronization. Carroll and Pecora [24] initially proposed the concept of synchronization in order to design the appropriate controllers to synchronize two chaotic systems with distinct initial conditions. There are variety of control strategies, such as active control, sliding mode control, adaptive control, and others. Complete synchronization, anti-synchronization, compound synchronization, difference synchronization and others have been developed to control the chaotic behaviors of chaotic systems [25-32]. Among all the control techniques for chaos synchronization, Linear feedback controller is simple in structure and easy to operate in practice. Many researchers have used the linear feedback controllers to synchronize and control chaos in various chaotic and hyperchaotic systems [33, 34]. Among them, the sliding mode control method is a variable structure control method, which has strong robustness in the face of external interference and parameter disturbance, and the theory of using sliding mode control to realize chaos synchronization has been studied more and more deeply. In 2014, Vaidyanathan and his collaborators used the sliding mode control method to realize global chaos synchronization of two identical three-dimensional chaotic systems [35] and they proposed a new sliding mode control method [36]. In 2023, Dinesh Khattar et al. [37] studied a sliding mode control problem of a three-dimensional chaotic system according to the sliding mode control method that proposed by Sundarapandian Vaidyanathan. Compared with the previous research [35-36], this paper extends the sliding mode control method from the three-dimensional chaotic system to the four-dimensional hyperchaotic system. These control techniques are too appealing and have been widely used due to their simplicity in configuration. In this paper, linear feedback control approach has been used to achieve the globally exponentially synchronization [38, 39] and Lyapunov stability theory ensure the global stability of the nonlinear systems. Since hyperchaotic systems have more complex dynamical behaviors and the sliding mode control method has the advantage of being insensitive to system parameters, this research has an important role in promoting the development of secure communication [32, 40].

The structure of this article is arranged as follows: Section 2 introduces a new nonlinear four-dimensional Lorenz system and discusses the dynamical behaviors of this system. Section 3 studies the global exponential attractive set of this system. Section 4 studies globally exponential synchronization through linear feedback controller. Section 5 studies synchronization through the sliding mode control method. Section 6 provides the conclusions of this paper.

2. Complex dynamics

2.1. System model and hyperchaotic attractor

In this paper, a new hyperchaotic system is proposed

$$\begin{cases} \dot{x} = a(y - x) + w, \\ \dot{y} = bx - xz - y, \\ \dot{z} = xy - cz, \\ \dot{w} = -x - dw, \end{cases} \quad (2.1)$$

where the parameters a, b, c, d are real constants of system (2.1). When the parameters $a = 10, b = 25, c = 3, d = 2$, system (2.1) is hyperchaotic. When the initial position of system (2.1) is selected as $(x_0, y_0, z_0, w_0) = (0.1, 0.2, 0.1, 0.2)$, then the three-dimensional hyperchaotic attractor of system (2.1) can be obtained, as shown in Figure 1. The evolution process of all variables over time t is shown in Figure 2.

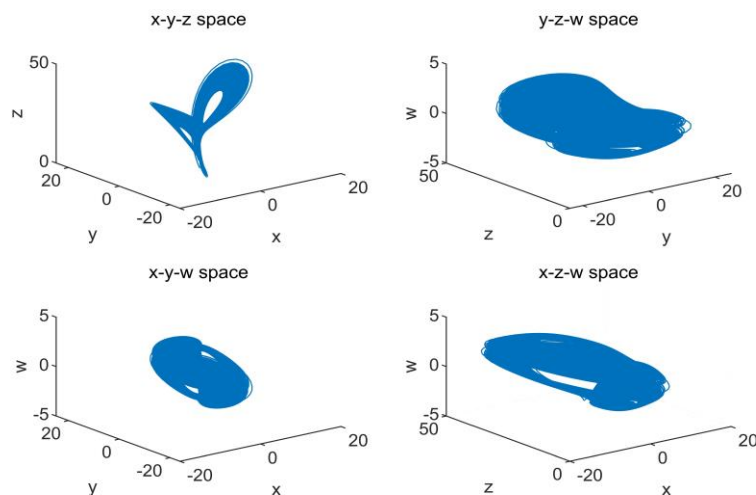


Figure 1. The hyperchaotic attractors of system (2.1) in the 3D space.

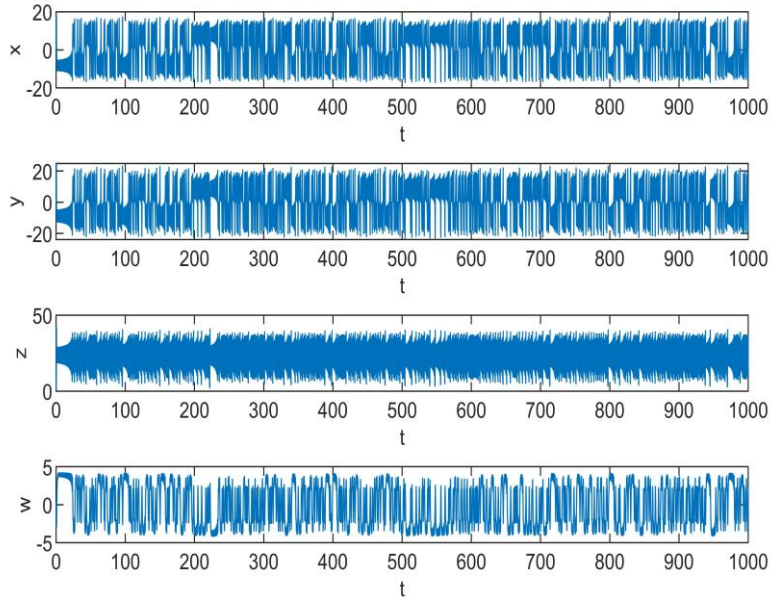


Figure 2. The evolution process of each variable of system (2.1) over the time t .

2.2. Dissipation

The vector field of system (2.1) is denoted as

$$F(x, y, z, w) = \begin{pmatrix} f_1(x, y, z, w) \\ f_2(x, y, z, w) \\ f_3(x, y, z, w) \\ f_4(x, y, z, w) \end{pmatrix} = \begin{pmatrix} a(y-x) + w \\ bx - xz - y \\ xy - cz \\ -x - dw \end{pmatrix}.$$

System (2.1) is dissipative under the condition $a + c + d + 1 > 0$, since we have

$$\nabla V = \frac{\partial f_1(x, y, z, w)}{\partial x} + \frac{\partial f_2(x, y, z, w)}{\partial y} + \frac{\partial f_3(x, y, z, w)}{\partial z} + \frac{\partial f_4(x, y, z, w)}{\partial w} = -(a + c + d + 1).$$

2.3. Fixed points and their stability

The fixed points of system (2.1) are determined by solving the following equations

$$\begin{cases} a(y-x) + w = 0, \\ bx - xz - y = 0, \\ xy - cz = 0, \\ -x - dw = 0. \end{cases} \quad (2.2)$$

Solving the above equation (2.2), the real equilibrium points of system (2.1) can be obtained as the following four cases:

- (i) If $a = 0, c \neq 0$, there is only one real fixed point $S_0 = (0, 0, 0, 0)$.

- (ii) If $a=0, c=0$, there are an infinite number of real fixed points.
 (iii) If $a \neq 0, c=0$, there are an infinite number of real fixed points.
 (iv) If $a \neq 0, c \neq 0$, then system (2.1) has only one real fixed point $S_0 = (0, 0, 0, 0)$ when $p = \frac{abcd - c(d+1)}{d^2(d+1)} \leq 0$. When $p = \frac{abcd - c(d+1)}{d^2(d+1)} \geq 0$, system (2.1) has the following three fixed points:

$$S_0 = (0, 0, 0, 0), S_+ = \left(-d\sqrt{p}, -\frac{(d+1)\sqrt{p}}{a}, bc - \frac{c(d+1)}{ad}, \sqrt{p} \right) \text{ and} \\ S_- = \left(d\sqrt{p}, \frac{(d+1)\sqrt{p}}{a}, bc - \frac{c(d+1)}{ad}, -\sqrt{p} \right).$$

In the following, we will study the stability of the fixed points of system (2.1) with parameters $a=10, b=25, c=3, d=2$. Consider the parameters of system (2.1) when $a=10, b=25, c=3, d=2$, which satisfies the second category in case (iv) above, so the system (2.1) has three fixed points. To study the stability of $S_0 = (0, 0, 0, 0)$, we will calculate the Jacobian matrix of system (2.1) at S_0 as follows:

$$J|_{S_0} = \begin{pmatrix} -10 & 10 & 0 & 1 \\ 25 & -1 & 0 & 0 \\ 0 & 0 & -3 & 0 \\ -1 & 0 & 0 & -2 \end{pmatrix}.$$

The eigenvalues of matrix $J|_{S_0}$ are calculated as $\lambda_1 = -21.9073$, $\lambda_2 = 10.9112$, $\lambda_3 = -2.0039$, and $\lambda_4 = -3$ by using computer software. Since there exists positive eigenvalue of matrix $J|_{S_0}$, so $S_0 = (0, 0, 0, 0)$ is an unstable fixed point of system (2.1). The stability analysis of S_+ and S_- by using the same method yields that S_+ and S_- are both stable fixed points of system (2.1).

2.4. Lyapunov exponents and Lyapunov dimension

When the parameters are selected as $a=10, b=25, c=3, d=2$, with the initial value $(x_0, y_0, z_0, w_0) = (0.1, 0.2, 0.1, 0.2)$, the Lyapunov exponent of system (2.1) is calculated as $\lambda_{L_1} = 0.8133$, $\lambda_{L_2} = 0.0036$, $\lambda_{L_3} = -2.0368$ and $\lambda_{L_4} = -14.7765$, respectively. And the Lyapunov dimension of the attractors of system (2.1) is calculated as [15, 16, 17]

$$D_L = j + \frac{\sum_{i=1}^j \lambda_{L_i}}{|\lambda_{L_{j+1}}|},$$

such that j is the largest integer that guarantees the inequality $\sum_{i=1}^j \lambda_{L_i} > 0$. And the Lyapunov dimension of system (2.1) in this case is

$$D_L = 2 + \frac{\lambda_{L_1} + \lambda_{L_2}}{|\lambda_{L_3}|} = 2.4011.$$

Since system (2.1) has two positive Lyapunov exponents, it indicates that system (2.1) is a hyperchaotic system. Moreover, the Lyapunov dimension of system (2.1) is positive fractional dimension, which indicates that the chaotic attractor of system (2.1) is fractional dimension. The Lyapunov exponent of system (2.1) is shown in Figure 3.

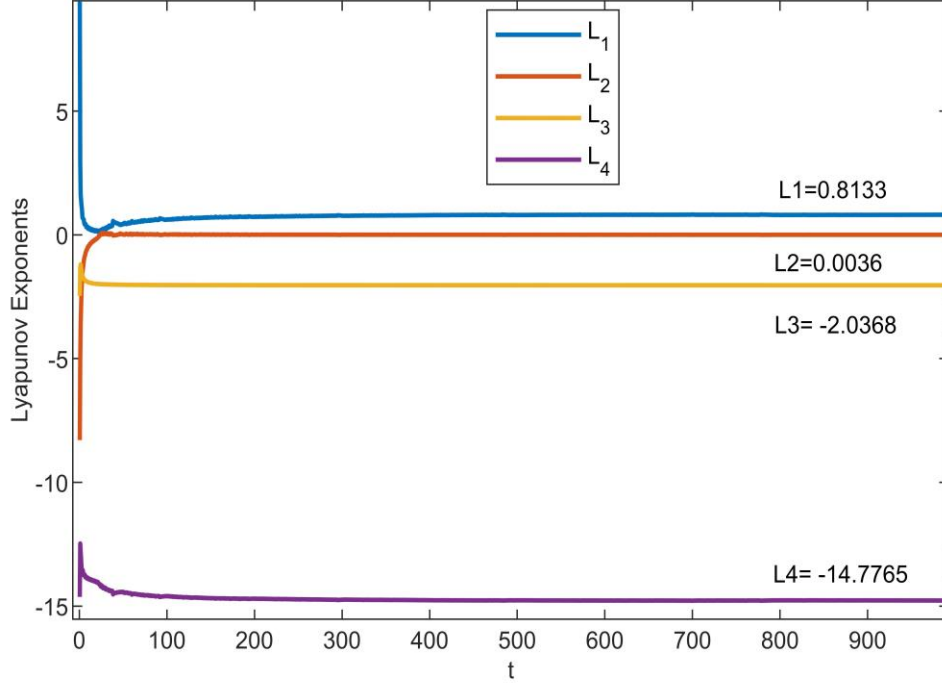


Figure 3. The Lyapunov exponent chart of system (2.1).

2.5. Effects of the changes in system parameters

If parameters $b = 25, c = 3, d = 2$ of system (2.1) are fixed, the value of parameter a is changed and the initial value $(x_0, y_0, z_0, w_0) = (0.1, 0.2, 0.1, 0.2)$ is fixed. When $a \in [0, 50]$, the Lyapunov exponents (LE) of system (2.1) with respect to parameter a can be obtained, as shown in Figure 4. The bifurcation diagram of the state variable x of system (2.1) with respect to parameter a is shown in Figure 5.

It can be found from Figure 4 that when $0 \leq a \leq 7.07$, the Lyapunov exponents of system (2.1) are all less than 0, and this system is in a stable state. When $7.07 < a < 11.05$, the largest Lyapunov exponent of the system is always greater than 0, and the system is in a chaotic state. However, there are also some points in small intervals corresponding to two positive Lyapunov exponents, so the system is in a hyperchaotic state. When $11.05 \leq a \leq 50$, the Lyapunov exponents of the system are all less than zero, except the smallest Lyapunov exponent, which is generally decreasing with the increase of a , and the other three Lyapunov exponents change very little, so the system is in a stable state. Observing the bifurcation diagram in Figure 5, the results of Figure 5 also confirm the above dynamical characteristics of this system.

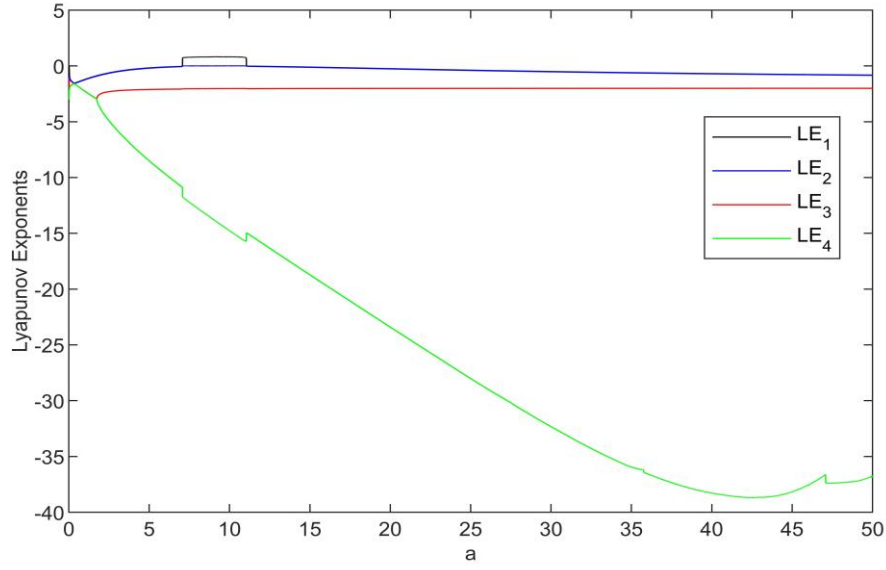


Figure 4. Lyapunov exponents diagram of system (2.1) with $a \in [0, 50]$.

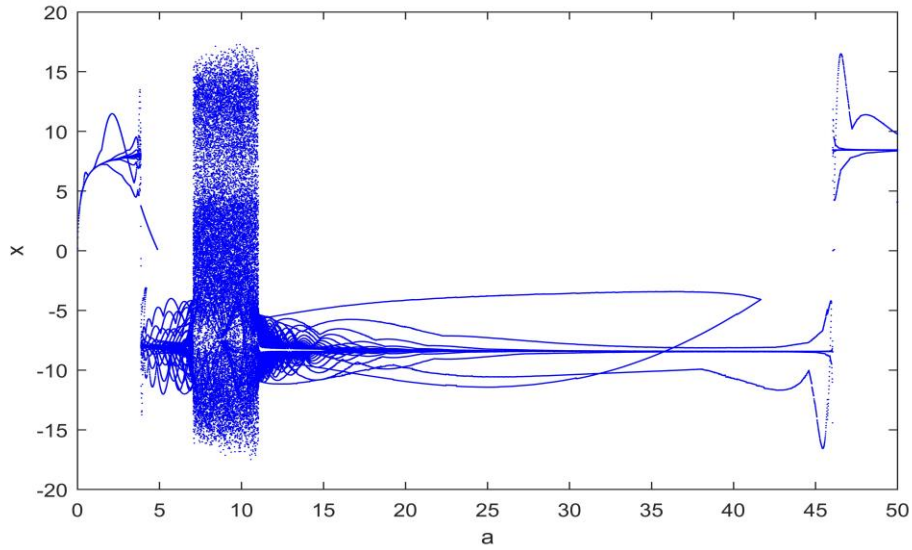


Figure 5. Bifurcation diagram of state variable x versus a .

If parameters $a = 10, c = 3, d = 2$ of system (2.1) are fixed, the value of parameter b is changed, and the initial value $(x_0, y_0, z_0, w_0) = (0.1, 0.2, 0.1, 0.2)$ is fixed. When $b \in [0, 50]$, the Lyapunov exponents of system (2.1) with respect to parameter b can be obtained, as shown in Figure 6. The bifurcation diagram of the state variable x of system (2.1) with respect to parameter b is shown in Figure 7.

It can be found from Figure 6 that when $0 \leq b \leq 24.55$, the Lyapunov exponents of system (2.1) are all less than 0, and the system is in a stable state. When $5 \leq b \leq 24.55$, the largest Lyapunov exponent and the second largest Lyapunov exponent of the system change in basically the same magnitude, and the third largest Lyapunov exponent is almost unchanged. When $24.55 < b \leq 50$, except for some points in small intervals,

system (2.1) basically has two Lyapunov exponents greater than 0, so the system is in a hyperchaotic state. These dynamical features of the system can also be observed from Figure 7.

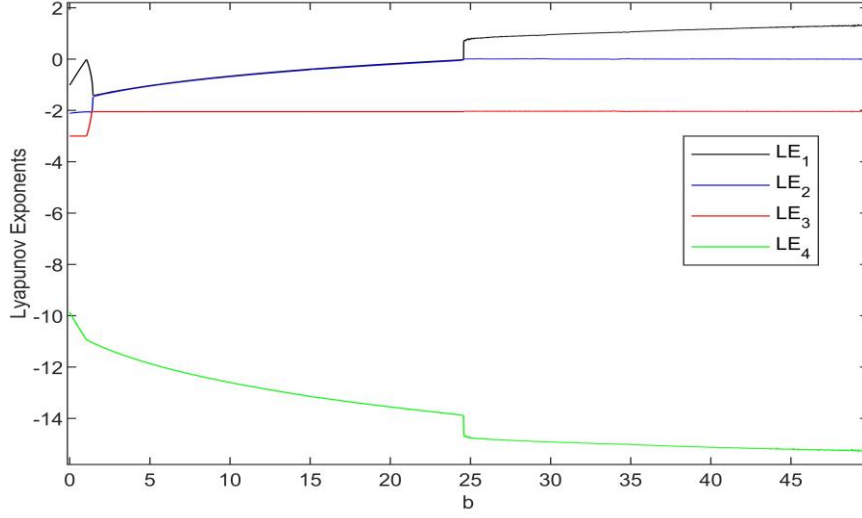


Figure 6. Lyapunov exponents diagram of system (2.1) with $b \in [0, 50]$.

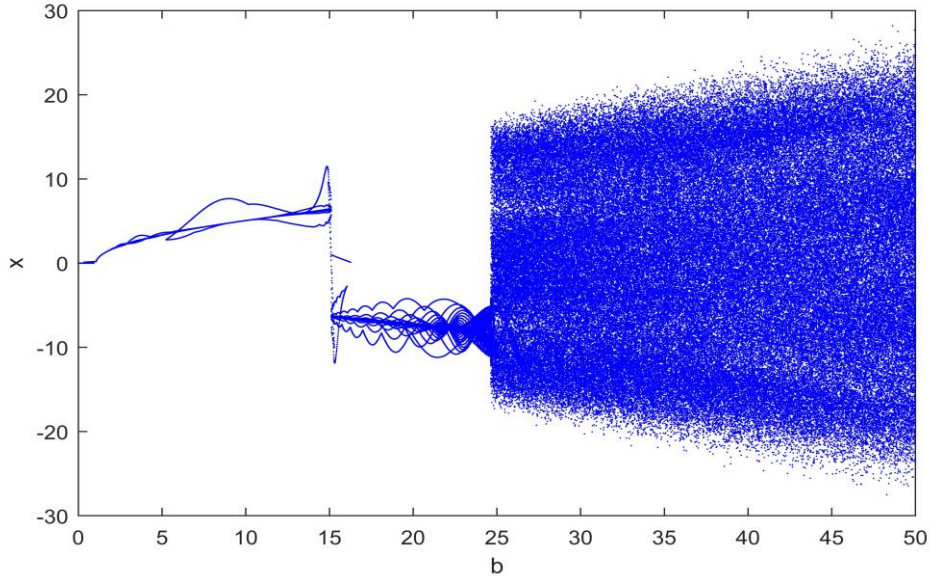


Figure 7. Bifurcation diagram of state variable x with respect to parameter b .

2.6. Sensitivity analysis to initial values

Parameters for system (2.1) are selected as $a = 10, b = 25, c = 3, d = 2$, and the initial value is $(x_0, y_0, z_0, w_0) = (0.1, 0.2, 0.1, 0.2)$. Let the initial value of the system (2.1) changes slightly. If the initial value of system (2.1) is changed into $(x_0, y_0, z_0, w_0) = (0.2, 0.3, 0.2, 0.3)$ for the first time and the initial value (x_0, y_0, z_0, w_0) of system (2.1) is changed into $(x_0, y_0, z_0, w_0) = (0.2, 0.3, 0.2, 0.3)$ for the second time,

then Matlab software is used to simulate the evolution of this system under three different initial values. The comparison diagram of the phase trajectory of this system with the initial value changing is shown in Figure 8. From the analysis of Figure 8, it can be found that even though the initial value of hyperchaotic system (2.1) has only a small change, the dynamical behavior of this system has a great difference, so this system is strongly sensitive to initial values.

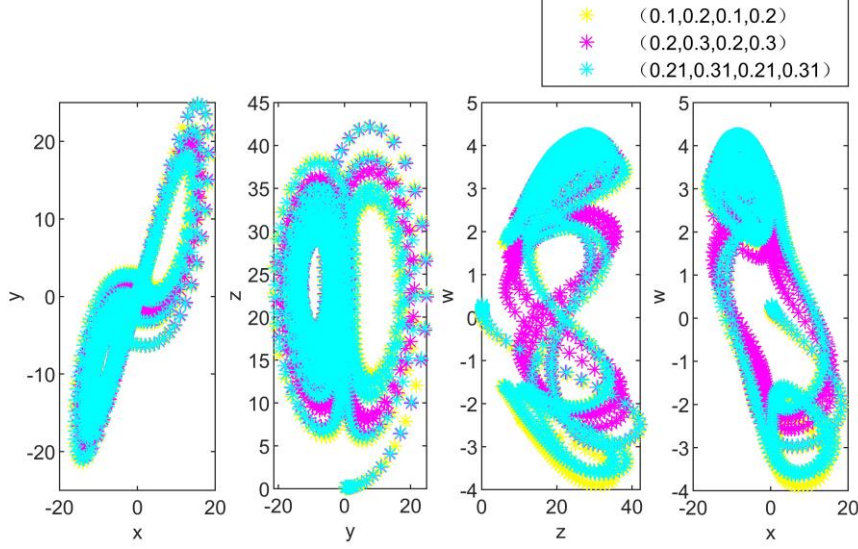


Figure 8. Initial value sensitivity map of system (2.1).

In the following part, we will study the globally exponential attractive set of hyperchaotic system (2.1) in order to provide theoretical basis for the control and synchronization of the hyperchaotic system (2.1).

3. Global exponential attractive set

Theorem 3.1.

Let $X(t) = (x(t), y(t), z(t), w(t))$, $X(t_0) = (x(t_0), y(t_0), z(t_0), w(t_0))$,

$M = \frac{(a+b)^2 c^2}{4c-2}$. When $V(X(t_0)) > M$, $V(X(t)) > M$ and $a > \frac{1}{2}, c > \frac{1}{2}, d > \frac{1}{2}, b > 0$,

we have the estimate of the exponential inequality with respect to the globally exponential attractive set of system (2.1)

$$[V(X(t)) - M] \leq [V(X(t_0)) - M] e^{-(t-t_0)}.$$

In particular,

$$\Omega = \{X \mid V(X) \leq M\} = \left\{X \mid x^2 + y^2 + (z-a-b)^2 + w^2 \leq \frac{(a+b)^2 c^2}{4c-2}\right\}$$

is the global exponential attractive set of system (2.1).

Proof. Construct

$$V(X) = V(x, y, z, w) = \frac{1}{2}[x^2 + y^2 + (z-a-b)^2 + w^2].$$

Let

$$F(x, y, z, w) = \left(\frac{1}{2} - a\right)x^2 - \frac{1}{2}y^2 + \left(\frac{1}{2} - c\right)z^2 + \left(\frac{1}{2} - d\right)w^2 + (a+b)(c-1)z + \frac{(a+b)^2}{2}.$$

And

$$\begin{aligned} \left. \frac{dV(X)}{dt} \right|_{(2.1)} &= x\dot{x} + y\dot{y} + (z-a-b)\dot{z} + w\dot{w}, \\ &= x[a(y-x) + w] + y[bx - xz - y] + (z-a-b)(xy - cz) + w(-x - dw), \\ &= -ax^2 - y^2 - cz^2 - dw^2 + (a+b)cz, \\ &= -V(X(t)) + \left(\frac{1}{2} - a\right)x^2 - \frac{1}{2}y^2 + \left(\frac{1}{2} - c\right)z^2 + \left(\frac{1}{2} - d\right)w^2 + (a+b)(c-1)z + \frac{(a+b)^2}{2}, \\ &= -V(X(t)) + F(X(t)). \end{aligned}$$

Let

$$\begin{cases} \frac{\partial F}{\partial x} = (1-2a)x = 0, \\ \frac{\partial F}{\partial y} = -y = 0, \\ \frac{\partial F}{\partial z} = (1-2c)z + (a+b)(c-1) = 0, \\ \frac{\partial F}{\partial w} = (1-2d)w = 0. \end{cases} \quad (3.1)$$

We can get the solution of the equation (3.1)

$$x = x_* = 0, y = y_* = 0, z = z_* = \frac{(a+b)(c-1)}{2c-1}, w = w_* = 0.$$

To find the maximum value of the function $F(x, y, z, w)$, the Hessian matrix of $F(x, y, z, w)$ at $P_0 = (x_*, y_*, z_*, w_*)$ can be obtained as

$$H_F(P_0) = \begin{pmatrix} \frac{\partial^2 F}{\partial x^2} & \frac{\partial^2 F}{\partial x \partial y} & \frac{\partial^2 F}{\partial x \partial z} & \frac{\partial^2 F}{\partial x \partial w} \\ \frac{\partial^2 F}{\partial y \partial x} & \frac{\partial^2 F}{\partial y^2} & \frac{\partial^2 F}{\partial y \partial z} & \frac{\partial^2 F}{\partial y \partial w} \\ \frac{\partial^2 F}{\partial z \partial x} & \frac{\partial^2 F}{\partial z \partial y} & \frac{\partial^2 F}{\partial z^2} & \frac{\partial^2 F}{\partial z \partial w} \\ \frac{\partial^2 F}{\partial w \partial x} & \frac{\partial^2 F}{\partial w \partial y} & \frac{\partial^2 F}{\partial w \partial z} & \frac{\partial^2 F}{\partial w^2} \end{pmatrix}_{P=P_0} = \begin{pmatrix} 1-2a & 0 & 0 & 0 \\ 0 & -1 & 0 & 0 \\ 0 & 0 & 1-2c & 0 \\ 0 & 0 & 0 & 1-2d \end{pmatrix}.$$

According to the extreme value theory of multivariate functions, $F(x, y, z, w)$ can obtain a maximum value at P_0 when the matrix $H_F(P_0)$ is a negative definite matrix. If the parameters of system (2.1) satisfy the following condition (3.2), the matrix $H_F(P_0)$ is a negative definite matrix.

$$\begin{cases} a > \frac{1}{2}, \\ c > \frac{1}{2}, \\ d > \frac{1}{2}. \end{cases} \quad (3.2)$$

Since $F(x, y, z, w)$ is quadratic and its local maximum is the global maximum, so

$$\sup_{X \in \mathbb{R}^4} F(X) = F(X) \Big|_{x=x_*, y=y_*, z=z_*, w=w_*} = \frac{(a+b)^2 c^2}{4c-2} = M. \quad (3.3)$$

Therefore,

$$\frac{dV(X(t))}{dt} \Big|_{(2.1)} \leq -V(X(t)) + M. \quad (3.4)$$

From the exponential inequality (3.4), we can get

$$[V(X(t)) - M] \leq [V(X(t_0)) - M] e^{-(t-t_0)}. \quad (3.5)$$

So, we can get

$$\overline{\lim}_{t \rightarrow +\infty} V(X(t)) \leq M,$$

which indicate that

$$\Omega = \{X \mid V(X) \leq G\} = \left\{ X \mid x^2 + y^2 + (z-a-b)^2 + w^2 \leq \frac{(a+b)^2 c^2}{4c-2} \right\}$$

is the global exponential attractive set of system (2.1).

The above Theorem 3.1 indicates that the trajectories of the system (2.1) are eventually attracted to a bounded region with an exponential rate, so that the trajectories of the system (2.1) are ultimately bounded. Hence, we can get the bounds of all variables of the hyperchaotic system (2.1) from the above theorem. The bounds of the variables of the hyperchaotic system (2.1) can be applied to study synchronization of two identical chaotic systems.

4. Global exponential synchronization

In the following, we firstly apply the linear controller to achieve global exponential synchronization with two identical hyperchaotic systems.

Assume the drive system is

$$\begin{cases} \dot{x}_1 = -ax_1 + ay_1 + w_1, \\ \dot{y}_1 = bx_1 - x_1 z_1 - y_1, \\ \dot{z}_1 = x_1 y_1 - cz_1, \\ \dot{w}_1 = -x_1 - dw_1. \end{cases} \quad (4.1)$$

And the response system is

$$\begin{cases} \dot{x}_2 = -ax_2 + ay_2 + w_2 - u_1, \\ \dot{y}_2 = bx_2 - x_2 z_2 - y_2 - u_2, \\ \dot{z}_2 = x_2 y_2 - cz_2 - u_3, \\ \dot{w}_2 = -x_2 - dw_2 - u_4. \end{cases} \quad (4.2)$$

Let $e_x = x_2 - x_1, e_y = y_2 - y_1, e_z = z_2 - z_1, e_w = w_2 - w_1$, then the error dynamical system

can be obtained as

$$\begin{cases} \dot{e}_x = -ae_x + ae_y + e_w - u_1(e_x, e_y, e_z, e_w), \\ \dot{e}_y = be_x - x_2z_2 + x_1z_1 - e_y - u_2(e_x, e_y, e_z, e_w), \\ \dot{e}_z = x_2y_2 - x_1y_1 - ce_z - u_3(e_x, e_y, e_z, e_w), \\ \dot{e}_w = -e_x - de_w - u_4(e_x, e_y, e_z, e_w), \end{cases} \quad (4.3)$$

where $u_i = u_i(e_x, e_y, e_z, e_w), i = 1, 2, 3, 4$ are four controllers that meet the conditions $u_i(0, 0, 0, 0) = 0, i = 1, 2, 3, 4$.

Theorem 4.1. The linear feedback control law

$$u_1 = k_1e_x, u_2 = k_2e_y, u_3 = k_3e_z, u_4 = k_4e_w, k_i \geq 0 (i = 1, 2, 3, 4)$$

can always be chosen such that the zero solution of system (4.3) is globally exponential stable, so that systems (4.1) and (4.2) achieve global exponential synchronization.

Proof. Define the radial unbounded vector Lyapunov function

$$V(X) = (|e_x|, |e_y|, |e_z|, |e_w|)^T$$

for system (4.3), and then its Dini derivative along the trajectory of system (4.3) is

$$\begin{aligned} D^+ |e_x| &\leq -(a + k_1)|e_x| + a|e_y| + |e_w|, \\ D^+ |e_y| &\leq (b + |z_1|)|e_x| - (1 + k_2)|e_y| + |x_2||e_z|, \\ D^+ |e_z| &\leq |y_1||e_x| + |x_2||e_y| - (c + k_3)|e_z|, \\ D^+ |e_w| &\leq -|e_x| - (d + k_4)|e_w|. \end{aligned}$$

The above inequality can be written as the following matrix

$$\begin{pmatrix} D^+ |e_x| \\ D^+ |e_y| \\ D^+ |e_z| \\ D^+ |e_w| \end{pmatrix} \leq \begin{pmatrix} -a - k_1 & a & 0 & 1 \\ b + |z_1| & -1 - k_2 & |x_2| & 0 \\ |y_1| & |x_2| & -c - k_3 & 0 \\ -1 & 0 & 0 & -d - k_4 \end{pmatrix} \begin{pmatrix} |e_x| \\ |e_y| \\ |e_z| \\ |e_w| \end{pmatrix} = C \bullet \begin{pmatrix} |e_x| \\ |e_y| \\ |e_z| \\ |e_w| \end{pmatrix}.$$

Let $C_i (i = 1, 2, 3, 4)$ be the i -order principal minor determinant of matrix C . If matrix C is a negative definite matrix, then the following condition (4.4) should be satisfied.

$$\begin{cases} C_1 = -a - k_1 < 0, \\ C_2 = \begin{vmatrix} -a - k_1 & a \\ b + |z_1| & -1 - k_2 \end{vmatrix} > 0, \\ C_3 = \begin{vmatrix} -a - k_1 & a & 0 \\ b + |z_1| & -1 - k_2 & |x_2| \\ |y_1| & |x_2| & -c - k_3 \end{vmatrix} < 0, \\ C_4 = |C| > 0. \end{cases} \quad (4.4)$$

Combined with Theorem 3.1, it can be seen that when the parameters a, b, c, d satisfy the condition (4.4), then there is the following exponential estimate of (4.1) and (4.2)

$$\frac{1}{2}[x_i^2 + y_i^2 + (z_i - a - b)^2 + w_i^2] \leq M, i = 1, 2.$$

Therefore, substituting the maximum

$\max_{x_i \in R} |x_i| = \sqrt{2M}, \max_{x_i \in R} |y_i| = \sqrt{2M}, \max_{x_i \in R} |z_i| = \sqrt{2M} + a + b, i = 1, 2$, into (4.4), we can obtain

$$\begin{cases} k_1 > -a, \\ k_2 > \frac{a(|z_1| + b)}{a + k_1} - 1, \\ k_3 > \frac{(a + k_1)|x_2|^2 + a|y_1||x_2|}{|C_2|} - c, \\ k_4 > \frac{|x_2|^2 - (1 + k_2)(c + k_3)}{-C_3} - d. \end{cases} \quad (4.5)$$

Therefore, when $k_i (i = 1, 2, 3, 4)$ satisfy the condition of (4.5), the matrix C can be guaranteed to be a negative definite matrix. Moreover, it can be seen from (4.5) that there exist a number of $k_i \geq 0 (i = 1, 2, 3, 4)$ such that (4.5) holds.

Hence, we have

$$D^+ (|e_x|, |e_y|, |e_z|, |e_w|)^T \leq C (|e_x|, |e_y|, |e_z|, |e_w|)^T. \quad (4.6)$$

Consider the comparing equation

$$\frac{d}{dt} (\alpha_1, \alpha_2, \alpha_3, \alpha_4)^T = C (\alpha_1, \alpha_2, \alpha_3, \alpha_4)^T.$$

From the above differential inequality (4.6), we can obtain

$$(\alpha_1(t), \alpha_2(t), \alpha_3(t), \alpha_4(t))^T = e^{C(t-t_0)} (\alpha_1(t_0), \alpha_2(t_0), \alpha_3(t_0), \alpha_4(t_0))^T, t \geq t_0.$$

Since the matrix C is a negative definite matrix, there exist $G \geq 1$ and $\beta > 0$ such that

$$|e^{C(t-t_0)}| \leq G e^{-\beta(t-t_0)}, t \geq t_0.$$

And since

$$(|e_x(t_0)|, |e_y(t_0)|, |e_z(t_0)|, |e_w(t_0)|)^T = (\alpha_1(t_0), \alpha_2(t_0), \alpha_3(t_0), \alpha_4(t_0))^T, t \geq t_0,$$

So, we have

$$\begin{aligned} \|(|e_x(t)|, |e_y(t)|, |e_z(t)|, |e_w(t)|)^T\| &\leq \|(\alpha_1(t), \alpha_2(t), \alpha_3(t), \alpha_4(t))^T\| \\ &\leq \|(\alpha_1(t_0), \alpha_2(t_0), \alpha_3(t_0), \alpha_4(t_0))^T\| G e^{-\beta(t-t_0)}. \end{aligned} \quad (4.7)$$

Notice that $(0, 0, 0, 0)$ is the zero solution of the error system (4.3). The above inequality (4.7) show that the zero solution of the error system (4.3) is global exponential stability, so system (4.1) and system (4.2) can achieve global exponential synchronization.

In the following part, we will perform numerical simulations to check the correctness of Theorem 4.1 in the paper. We will give numerical simulations of global exponential synchronization for $a = 10, b = 25, c = 3, d = 2$ and the initial conditions of the drive system and the response system at $t_0 = 0$ are selected as

$$(x_1(0), y_1(0), z_1(0), w_1(0)) = (1, 3.5, 0.5, 4), (x_2(0), y_2(0), z_2(0), w_2(0)) = (4, 0.3, 3, 0.5).$$

Choose $k_1 = 10, k_2 = 53, k_3 = 6350, k_4 = 2$, then Theorem 4.1 can be satisfied. The diagram of linear synchronization process between system (4.1) and (4.2) is shown in

Figure 9.

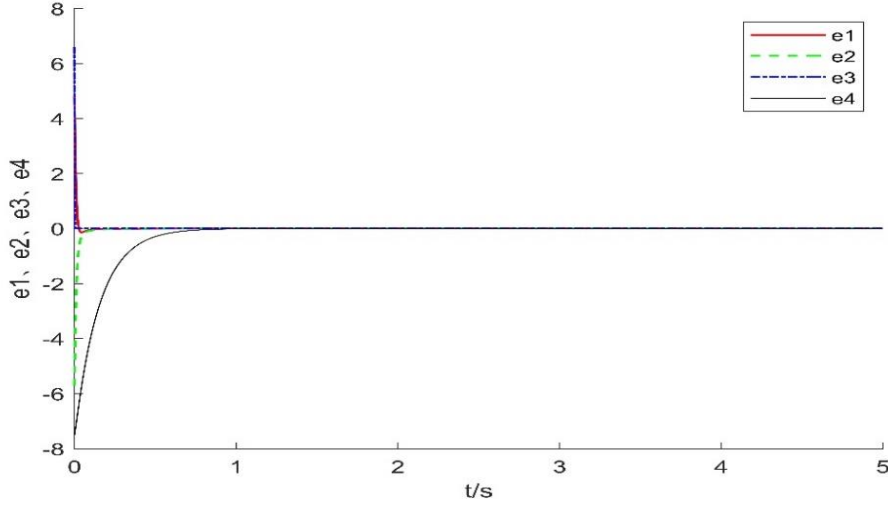


Figure 9. Synchronization of linear feedback control is illustrated for $k_1 = 10, k_2 = 53, k_3 = 6350, k_4 = 2$.

From Figure 9, we can see that the oscillations of the drive and response systems rapidly become totally indistinguishable which indicate that synchronization is achieved very quickly.

The simulation results show that the linear feedback method can make system (4.1) and (4.2) achieve global exponential synchronization very quickly, which confirms that the linear feedback method is very effective.

Next, we will apply sliding mode control method to system (2.1) to achieve globally asymptotical synchronization. Suppose (4.1) is still selected as the transmitting system and (4.2) as the receiving system and a controller will be designed to make systems (4.1) and (4.2) achieve globally asymptotical synchronization. We have the following results for the sliding mode control.

5. Sliding mode control of synchronization

Theorem 5.1. The parameters $a = 10, b = 25, c = 3, d = 2$ are selected for system (4.1) and system (4.2), and the controller is designed as $u = \varphi(x_1, y_1, z_1, x_2, y_2, z_2) - Qv$,

$$\text{where } u = \begin{pmatrix} u_1 \\ u_2 \\ u_3 \\ u_4 \end{pmatrix}, \quad \varphi(x_1, y_1, z_1, x_2, y_2, z_2) = \begin{pmatrix} 0 \\ x_1 z_1 - x_2 z_2 \\ x_2 y_2 - x_1 y_1 \\ 0 \end{pmatrix}, \quad Q = \begin{pmatrix} 1 \\ 1 \\ 1 \\ 1 \end{pmatrix} \text{ and } v \text{ is the sliding}$$

mode controller. And when

$$v = -0.5e_1 - 10e_2 - 3.5e_3 + 3e_4 - 5(2e_1 + e_3 - e_4)^2 \operatorname{sgn}(2e_1 + e_3 - e_4),$$

system (4.1) and system (4.2) can achieve globally asymptotical synchronization under any initial states $(x_1(0), y_1(0), z_1(0), w_1(0))$ and $(x_2(0), y_2(0), z_2(0), w_2(0))$.

Proof. Define a new control signal as

$$u = \varphi(x_1, y_1, z_1, x_2, y_2, z_2) - Qv \quad (5.1)$$

where $u = \begin{pmatrix} u_1 \\ u_2 \\ u_3 \\ u_4 \end{pmatrix}$, $\varphi(x_1, y_1, z_1, x_2, y_2, z_2) = \begin{pmatrix} 0 \\ x_1 z_1 - x_2 z_2 \\ x_2 y_2 - x_1 y_1 \\ 0 \end{pmatrix}$, $Q = \begin{pmatrix} 1 \\ 1 \\ 1 \\ 1 \end{pmatrix}$ and v is the sliding

mode controller. Then the error dynamical system (4.3) can be transformed into the following matrix form:

$$\dot{e} = De + \varphi(x_1, y_1, z_1, x_2, y_2, z_2) - u. \quad (5.2)$$

where $e = \begin{pmatrix} e_1 \\ e_2 \\ e_3 \\ e_4 \end{pmatrix}$ and $D = \begin{pmatrix} -a & a & 0 & 1 \\ b & -1 & 0 & 0 \\ 0 & 0 & -c & 0 \\ -1 & 0 & 0 & -d \end{pmatrix}$.

The sliding variable can be chosen to be $S(e) = Re = 2e_1 + e_3 - e_4$, where $R = (2, 0, 1, -1)$.

Let E be the identity matrix and the parameters of hyperchaotic system (2.1) are chosen as $a = 10, b = 25, c = 3, d = 2$, then the eigenvalues of the matrix

$T = [E - Q(RQ)^{-1}R]D$ can be calculated as $\eta_1 = 0, \eta_2 = -1, \eta_3 = -1.5, \eta_4 = -3$. According to the literature [35], it can be shown that the sliding manifold is globally asymptotically stable.

According to Vaidyanathan's theorem in the paper [36], sliding mode control v can be defined as

$$v(t) = -(RQ)^{-1}[R(kE + D)e + qS^2 \operatorname{sgn}(S)]. \quad (5.3)$$

where k and q are sliding constants and $\operatorname{sgn}(S)$ is a sign function with respect to S .

The error dynamical system (5.2) can be written as the following form according to (5.1) and (5.3)

$$\dot{e} = De - Q(RQ)^{-1}[R(kE + D)e + qS^2 \operatorname{sgn}(S)]. \quad (5.4)$$

Define the Lyapunov function $V(e) = \frac{1}{2}S^2(e)$. The equation of sliding mode motion can be expressed by $S(e) = 0$, and $\dot{S}(e) = 0$. Differentiate $V(e)$ with respect to t along the trajectory of the system (5.4)

$$\begin{aligned} \left. \frac{dV(e)}{dt} \right|_{(5.4)} &= S \cdot \dot{S}(e), \\ &= SR\dot{e}, \\ &= SR\{De - Q(RQ)^{-1}[R(kE + D)e + qS^2 \operatorname{sgn}(S)]\}, \\ &= S(-kERe - qS^2 \operatorname{sgn}(S)), \\ &= -kS^2 - qS^3 \operatorname{sgn}(S), \\ &< 0. \end{aligned}$$

Thus, the zero solution of the error system (5.2) is globally asymptotically stable, indicating that system (4.1) and system (4.2) can achieve globally asymptotical synchronization.

When the sliding constants k, q are chosen as $k = 10$ and $q = 10$, it can be obtained

$$v = -0.5e_1 - 10e_2 - 3.5e_3 + 3e_4 - 5(2e_1 + e_3 - e_4)^2 \operatorname{sgn}(2e_1 + e_3 - e_4). \quad (5.5)$$

Compared with the previous research [36-37], this paper extends the sliding mode control method from the three-dimensional chaotic system to the four-dimensional hyperchaotic system. Since hyperchaotic systems have more complex dynamical behaviors and the sliding mode control method has the advantage of being insensitive to parameter changes, this research has an important role in promoting the development of secure communication.

In order to verify the correctness of the above theory, we will give some numerical simulations in the following part. In this section, we will give numerical simulations of the sliding mode synchronization for $a = 10, b = 25, c = 3, d = 2$ and the initial conditions of the drive system and the response system at $t_0 = 0$ are selected as

$$(x_1(0), y_1(0), z_1(0), w_1(0)) = (1, 3.5, 0.5, 4), (x_2(0), y_2(0), z_2(0), w_2(0)) = (4, 0.3, 3, 0.5).$$

Choose $k = 10, q = 10$, then the above Theorem 5.1 can be satisfied. The sliding mode synchronization of this hyperchaotic system is shown in Figure 10.

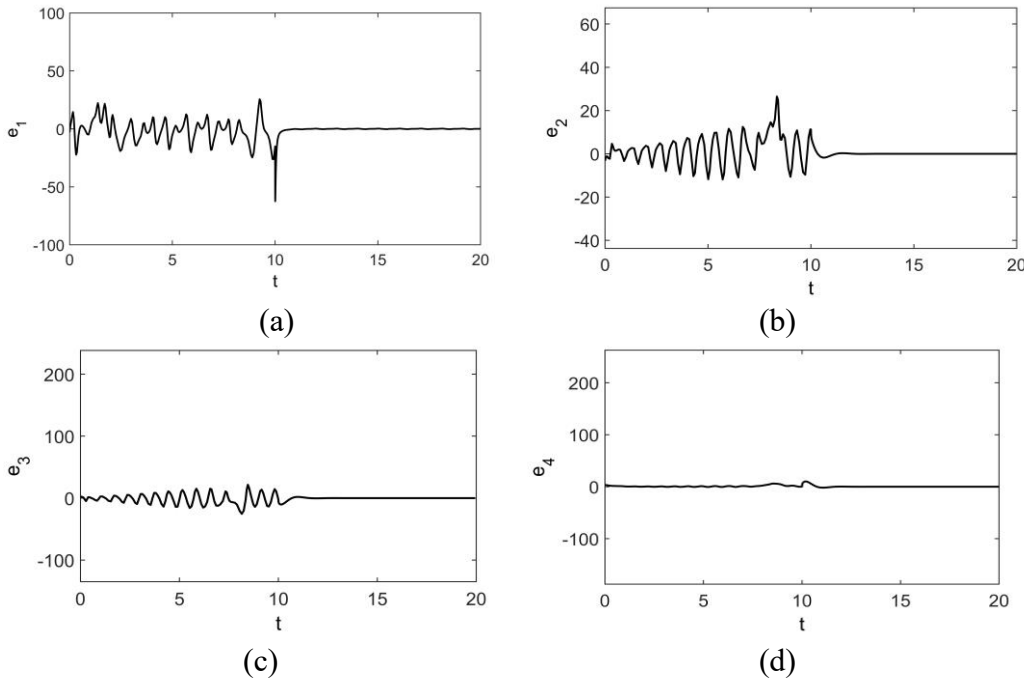


Figure 10. Synchronization of sliding mode control is illustrated when $k = 10, q = 10$.

From Figure 10, we can see that the oscillations of the drive and response systems rapidly become totally indistinguishable which indicate that synchronization is achieved very quickly.

The simulations show that the sliding mode control method can both make system (4.1) and system (4.2) achieve synchronization very quickly, which confirms that the sliding mode control methods is very effective.

6. Conclusions

In this paper, a new four-dimensional hyperchaotic system is proposed and analyzed by using chaos theory and numerical simulations. The three-dimensional phase diagram and time sequence diagrams of each variable of this hyperchaotic system are drawn by the computer software. The influences of parameters a and b for this hyperchaotic system are also analyzed. The sensitivity of this system to the initial value is also analyzed. Then, by using Lyapunov-like function method, the global exponential attractive set of this system is also obtained. Then by using the result of the global exponential attractive set, it is proved that this system can achieve global exponential synchronization by applying linear feedback controllers, and the lower bound of linear feedback controller is calculated. Then, a suitable sliding mode controller is used to realize globally asymptotical synchronization for this new hyperchaotic system. Finally, two control methods are simulated by numerical simulations and the simulations show that both control methods are effective. The linear control method has the advantage of simple structure and it is easy to design in practical application. The sliding mode controller has the characteristics of simple design, insensitive to parameter disturbance and external interference and strong robustness.

Acknowledgments

We will thank professor Shutang Liu in Shandong University of China, professor Jinde Cao in Southeast University of China, professor Jinhua Lu in Beihang University (also at Chinese Academy of Sciences) and Professor Guanrong Chen in the City University of Hong Kong for their help with us. We also thank Professor Miguel A. F. Sanjuan in the Spanish Royal Academy of Sciences (also at Universidad Rey Juan Carlos of Spain) for his support. Finally, the authors will thank the anonymous reviewers for their careful reading and useful suggestions, which greatly improved the presentation of this paper. Without the help of the reviewers, this paper would not be at this level.

Data availability statement

Data sharing not applicable to this article as no datasets were generated or analysed during the current study.

Declaration of interests

The authors that reported in this paper have no conflicts of interest.

References

- [1] H. Poincaré, Sur le probleme des trois corps et les equations de la dynamique, *Acta Math.*, 1890, 13, 1-270.
- [2] T. Li and J. Yorke, Period three implies chaos, *Am. Math. Mon.*, 1975, 82(10), 985-992.
- [3] E. Lorenz, Deterministic nonperiodic flow, *J. Atmos. Sci.*, 1963, 20, 130-141.
- [4] O. E. Rossler, An equation for continuous chaos, *Phys. Lett. A*, 1976, 57 397-398.
- [5] L. Chua, M. Komuro and T. Matsumoto, The double scroll family, *IEEE Trans.*

- Circuits Syst., 1986, 33(11), 1072-1118.
- [6] N. Kuznetsov, T. Mokaev, V. Ponomarenko, E. Seleznev, N. Stankevich and L. Chua, Hidden attractors in Chua circuit: Mathematical theory meets physical experiments, *Nonlinear Dyn.*, 2023, 111(6), 5859–5887.
 - [7] L. Stenflo, Generalized Lorenz equations for acoustic-gravity waves in the atmosphere, *Phys. Scr.*, 1996, 3, 83–84.
 - [8] G. Chen and T. Ueta, Yet another chaotic attractor, *Int. J. Bifurc. Chaos Appl. Sci. Eng.*, 1999, 9(7), 1465–1466.
 - [9] J. Lu and G. Chen, A new chaotic attractor coined, *Int. J. Bifurc. Chaos Appl. Sci. Eng.*, 2002, 12(3), 659–661.
 - [10] J. Lu, G. Chen, D. Cheng and S. Celikovsky, Bridge the gap between the Lorenz system and the Chen system, *Int. J. Bifurc. Chaos Appl. Sci. Eng.*, 2002, 12(12), 2917-2926.
 - [11] M. P. Asir, K. Thamilmaran, A. Prasad, U. Feudel, N.V. Kuznetsov and M. D. Shrimali, Hidden strange nonchaotic dynamics in a non-autonomous model, *Chaos Solit. Fract.*, 2023, 168, 113101.
 - [12] G. M. Mahmoud, M. A. Al-Kashif and A. A. Farghaly, Chaotic and hyperchaotic attractors of a complex nonlinear system, *J. Phys. A: Math. Theor.*, 2008, 41(5), 055104.
 - [13] P. Frederickson, J. Kaplan, E. Yorke and J. Yorke, The Lyapunov dimension of strange attractors, *J. Differ. Equ.*, 1983, 49(2), 185–207.
 - [14] C. Sparrow, *The Lorenz Equations, Bifurcations, Chaos and Strange Attractors*, Applied Mathematical Science, vol. 41, Springer, New York, 1982.
 - [15] A. Wolf, J. B. Swift, H. L. Swinney, J. A. Vastano, Determining Lyapunov exponents from a time series, *Physica D.*, 1985, 16(3), 285–317.
 - [16] J. C. Vallejo and M. Sanjuan, *Predictability of Chaotic Dynamics, A finite-time Lyapunov exponents approach*, Springer, Cham, 2019.
 - [17] F. Zhang, P. Zhou and F. Xu, Qualitative properties of a physically extended six-dimensional Lorenz system, *Int. J. Bifurc. Chaos Appl. Sci. Eng.*, 2024, 34(7), 2450083.
 - [18] F. Zhang, X. Liao, G. Zhang and C. Mu, Dynamical analysis of the generalized Lorenz systems, *J. Dyn. Control Syst.*, 2017, 23(2), 349–362.
 - [19] G. Leonov and V. Boichenko, Lyapunov’s direct method in the estimation of the Hausdorff dimension of attractors, *Acta Appl. Math.*, 1992, 26(1), 1–60.
 - [20] F. Zhang, X. Liao and G. Zhang, Some new results for the generalized Lorenz system, *Qual. Theory Dyn. Syst.*, 2017, 16(3), 749–759.
 - [21] F. Zhang and G. Zhang, Further results on ultimate bound on the trajectories of the Lorenz system, *Qual. Theory Dyn. Syst.*, 2016, 15(1), 221-235.
 - [22] N. Kuznetsov, T. Mokaev, O. Kuznetsova, et al., The Lorenz system: hidden boundary of practical stability and the Lyapunov dimension, *Nonlin. Dyn.*, 2020, 102, 713–732.
 - [23] X. Zhang, J. Liu, J. Liang, D. Wang and Y. Sun, Chaos anti-control of coexisting infinite signals and pinning synchronization of a complex-valued laser chain network, *Eur. Phys. J. Plus*, 2024, 139(1), 65.
 - [24] T. L. Carroll and L. M. Pecora, Synchronizing chaotic circuits, *IEEE Trans. Circuits Syst.*, 1991, 38(4), 453-456.

- [25] M. G. Rosenblum, A. S. Pikovsky and J. Kurths, Phase synchronization in driven and coupled chaotic oscillators, *IEEE Trans. Circuits Syst.*, 1997, 44(10), 874-881.
- [26] H. Nijmeijer, A dynamical control view on synchronization, *Physica D.*, 2001, 154(3-4), 219-228.
- [27] W. W. Ho and S. Choi, Exact emergent quantum state designs from quantum chaotic dynamics, *Phys. Rev. Lett.*, 2022, 128(6), 060601.
- [28] M. Mohadeszadeh and N. Pariz, An application of adaptive synchronization of uncertain chaotic system in secure communication systems, *Int. J. Simul. Model.*, 2022, 42(1), 143-152.
- [29] X. Zhao, J. Liu, G. Chen, L. Chai and D. Wang, Dynamics and synchronization of complex-valued ring networks, *Int. J. Bifurc. Chaos Appl. Sci. Eng.*, 2022, 32(5), 2230011.
- [30] J. S. Kim, D. H. Kim, J. H. Lee and J. S. Lee, Smooth pulse number transition strategy considering time delay in synchronized SVPWM, *IEEE Trans. Power Electron.*, 2022, 38(2), 2252-2261.
- [31] S. Zhou, Y. C. Lai and W. Lin, Stochastically adaptive control and synchronization: From globally one-sided Lipschitzian to only locally Lipschitzian systems, *SIAM J. Appl. Dyn. Syst.*, 2022, 21(2), 932-959.
- [32] M. Liu, J. Liu, J. Liang, Y. Sun and Y. Shu, Observer-based secure synchronization control of directed complex-valued dynamical networks under link attacks, *Nonlinear Dyn.*, 2024, 112, 12303-12318.
- [33] G. Laarem, A new 4-D hyper chaotic system generated from the 3-D Rössler chaotic system, dynamical analysis, chaos stabilization via an optimized linear feedback control, it's fractional order model and chaos synchronization using optimized fractional order sliding mode control, *Chaos Soliton. Fract.*, 2021, 152, 111437.
- [34] S. C. Sinha, J. T. Henrichs and B. Ravindra, A general approach in the design of active controllers for nonlinear systems exhibiting chaos, *Int. J. Bifurc. Chaos Appl. Sci. Eng.*, 2000, 10(1), 165-178.
- [35] S. Vaidyanathan, Global chaos synchronization of identical Li-Wu chaotic systems via sliding mode control, *Int. J. Model. Identif. Control*, 2014, 22(2), 170-177.
- [36] S. Vaidyanathan, S. Sampath and A.T. Azar, Global chaos synchronisation of identical chaotic systems via novel sliding mode control method and its application to Zhu system, *Int. J. Model. Identif. Control*, 2015, 23(1), 92-100.
- [37] D. Khattar, N. Agrawal and G. Singh, Chaos synchronization of a new chaotic system having exponential term via adaptive and sliding mode control, *Differ. Equ. Dyn. Syst.*, 2023, <https://doi.org/10.1007/s12591-023-00635-0>.
- [38] F. Zhang, F. Xu and X. Zhang, Qualitative behaviors of a four-dimensional Lorenz system, *J. Phys. A: Math. Theor.*, 2024, 57(9), 095201.
- [39] F. Zhang, X. Liao, C. Mu, G. Zhang and Y. Chen, On global boundedness of the Chen system, *Discrete Contin. Dyn. Syst., Ser. B.*, 2017, 22(4), 1673-1681.
- [40] H. Fujisaka and T. Yamada, Stability theory of synchronized motion in coupled-oscillator systems, *Prog. Theor. Phys.*, 1983, 69(1), 32-47.